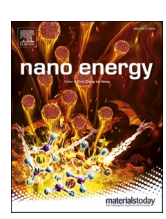
ELSEVIER

Contents lists available at ScienceDirect

# Nano Energy

journal homepage: www.elsevier.com/locate/nanoen





# Rational catalyst structural design to facilitate reversible Li-CO<sub>2</sub> batteries with boosted CO<sub>2</sub> conversion kinetics

Shiming Chen <sup>a,1</sup>, Kai Yang <sup>b,\*,1</sup>, Hengyao Zhu <sup>a</sup>, Jianan Wang <sup>c</sup>, Yi Gong <sup>b</sup>, Huanxin Li <sup>d</sup>, Manman Wang <sup>b</sup>, Wenguang Zhao <sup>a</sup>, Yuchen Ji <sup>a</sup>, Feng Pan <sup>a</sup>, S. Ravi P. Silva <sup>b</sup>, Yunlong Zhao <sup>e,f,\*\*</sup>, Luyi Yang <sup>a,\*</sup>

- <sup>a</sup> School of Advanced Materials, Peking University, Shenzhen Graduate School, Shenzhen 518055, China
- <sup>b</sup> Advanced Technology Institute, University of Surrey, Guildford, Surrey GU2 7XH, UK
- <sup>c</sup> Department of Environmental Science and Engineering, State Key Laboratory of Multiphase Flow in Power Engineering, Xi'an Jiaotong University, 28 Xianning West Road, Xi'an 710049, China
- <sup>d</sup> Department of Engineering, University of Cambridge, 9 JJ Thomson Avenue, Cambridge CB3 0FA, UK
- e Dyson School of Design Engineering, Imperial College London, London SW7 2BX, UK
- <sup>f</sup> National Physical Laboratory, Teddington, Middlesex TW11 OLW, UK

### ARTICLE INFO

### Keywords: Li-CO<sub>2</sub> battery CO<sub>2</sub> conversion Joule heating Electrocatalyst Pouch cell

### ABSTRACT

Lithium-CO $_2$  batteries (LCBs) are regarded as a promising energy system for CO $_2$  drawdown and energy storage capability which has attracted widespread interest in carbon neutrality and sustainable societal development. However, their practical application has been limited by slow kinetics in catalytic reactions and poor reversibility of Li $_2$ CO $_3$  products which leads to the issue of a large overpotential, low energy efficiency and poor reversibility. Herein, an efficient catalyst design and synthesis strategy is proposed to overcome the abovementioned bottleneck. Through an electrical joule heating procedure, Pt with random crystal orientations is converted into a 3D porous Pt catalyst with preferred (111) crystal orientation within seconds, exhibiting enhanced CO $_2$  conversion kinetics with superior electrochemical performance. This includes ultralow overpotential (0.45 V), fast rate charging (up to 160  $\mu$ A cm $^{-2}$ ) and high stability (over 200 cycles under 40  $\mu$ A cm $^{-2}$ ). A proof-of-concept stacked Li-CO $_2$  pouch cell, with stable operation under practical current density is demonstrated, indicating significant potential for large-scale operations. This bottom-up design of efficient catalysts and synthesis strategy offers a rapid and cost-effective approach to maximizing catalytic sites for CO $_2$  conversion under restricted catalyst loading, showcasing its versatility across a broad spectrum of catalyst-based energy conversion and storage systems.

# 1. Introduction

The massive consumption of non-renewable fossil fuels has caused increasingly energy shortage issues and corresponding  $CO_2$  emissions also trigger serious environmental crises such as global warming and extreme climate change [1,2]. New negative emissions technologies to both address the ever-increasing energy demand and reduce  $CO_2$  emissions are of great importance for carbon neutrality and the sustainable development of human society [3,4]. Among the novel carbon dioxide capture and utilization technologies (e.g.,  $CO_2$  reduction techniques)

[5–7], metal-CO<sub>2</sub> batteries have attracted considerable attention due to their unique characteristic of CO<sub>2</sub> recyclability and providing green energy storage simultaneously [8,9]. With CO<sub>2</sub> as the reactant, rechargeable Li-CO<sub>2</sub> batteries (LCBs) deliver a high theoretic energy density of 1876 Wh/kg and theoretical equilibrium potential at ~2.8 V (vs. Li/Li<sup>+</sup>, based on the reaction of 3CO<sub>2</sub> + 4Li  $\leftrightarrow$  2Li<sub>2</sub>CO<sub>3</sub> + C), which is substantially higher than that of high-energy lithium-ion battery systems (e.g., ~300 Wh/kg of Si-graphite//NCM systems). The direct utilization of CO2 in energy conversion and storage devices also provide effective approaches for the sustainable development of carbon neutral

<sup>\*</sup> Corresponding authors.

<sup>\*\*</sup> Corresponding author at: Dyson School of Design Engineering, Imperial College London, London SW7 2BX, UK. E-mail addresses: kai.yang@surrey.ac.uk (K. Yang), yunlong.zhao@imperial.ac.uk (Y. Zhao), yangly@pkusz.edu.cn (L. Yang).

<sup>&</sup>lt;sup>1</sup> These authors contributed equally to this work.

S. Chen et al. Nano Energy 117 (2023) 108872

society. These advantages make LCBs as promising next-generation energy storage devices not only for substitution of conventional Li-ion batteries but also extended application in aerospace exploration (especially on predominant CO<sub>2</sub> environments, such as Mars) [10].

Despite being very promising and extensively investigated since its emergence, the widespread applications of LCBs still suffer from several thorny research bottlenecks. The sluggish CO<sub>2</sub> conversion leads to large overpotential (> 1 V), low energy efficiency (< 75 %) and inferior rate performance (normally operated at 0.1 C) [10,11]. The poor reversibility caused by the incomplete decomposition of insulating  $\rm Li_2CO_3$  products and the unexpected side reactions (e.g. electrolyte decomposition, carbon corrosion, etc. at high charging potentials) leads to limited cycle life [12,13]. The lack of rational electrode and electrocatalyst structure design fails to ensure large-scale practical application and exhibits uncompetitive areal capacity (< 1 mAh cm<sup>-2</sup>) [14]. Therefore,

the key challenge to promote LCBs performance lies in the development of highly efficient cathode electrocatalysts. To this end, tremendous efforts have been devoted to investigating various electrocatalysts such as carbon-based materials (graphene, carbon nanotubes, carbon aerogel, porous activated carbon, etc.), transition metal compounds (oxide, sulphide, carbide, etc.), and noble metal/alloys (Pt, Ir, Ru, etc.) [8,10,12]. Despite efforts to improve electrochemical performance, many electrocatalysts have not yet demonstrated satisfactory results when evaluated under practical operating conditions such as higher operating current density and larger electrode size.

On the other hand, achieving a balance between long-term durability, high catalytic performance, and cost control remains a challenge [10,12]. For instance, the development of single-atom electrocatalysts has been pursued to reduce costs, but some have exhibited susceptibility to side reaction chemicals (e.g., carbon monoxide) during  $CO_2$ 

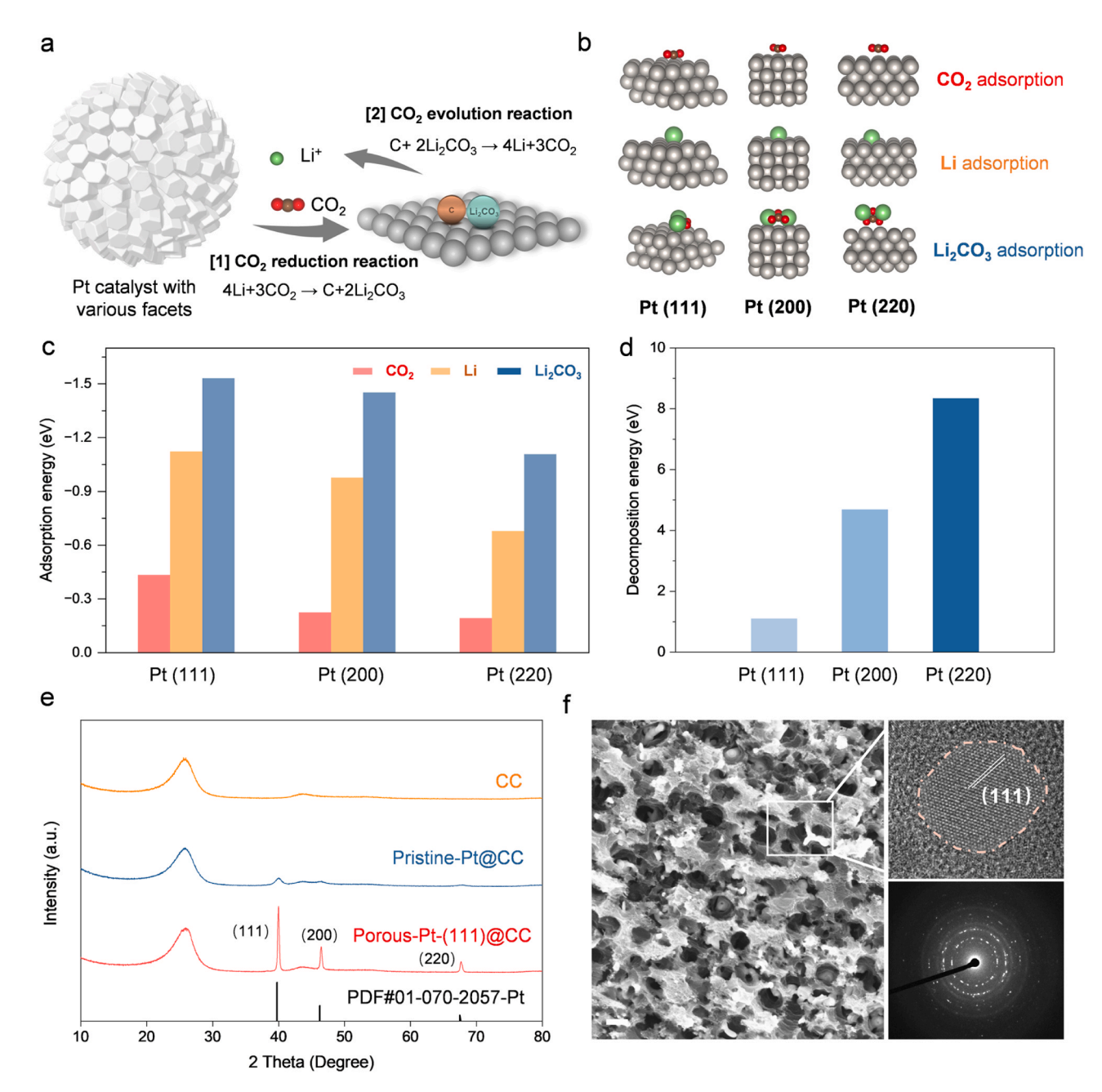


Fig. 1. Design and characterizations of Pt electrocatalyst. (a) Schematic  $CO_2$  conversion process in Pt-based LCBs. (b) Side view of adsorption behaviour of  $CO_2$ , Li and  $Li_2CO_3$  on different orientations of Pt surface and (c) comparison of corresponding adsorption energy. (d) Decomposition energy of  $Li_2CO_3$  on different orientations of Pt surface. (e) XRD analysis of different electrodes. (f) Detailed surface structure and TEM observation of the electrode after HTS (scale bar = 200 nm).

conversion, leading to structural damage and limited cycle life [15–21]. Additionally, incomplete exposure of catalytic sites for  $\mathrm{CO}_2$  conversion can result in suboptimal rate performance [16,22]. Thus, designing catalysts with an optimal crystal structure to maximize catalytic sites for  $\mathrm{CO}_2$  conversion is a critical principle to consider.

Herein, we demonstrate an efficient modulation strategy of the catalyst structure to enhance CO2 conversion kinetics and improve the overall electrochemical performance of LCBs. Following the theoretic simulations on the preferred Pt facet for LCBs reactions, electrical Joule heating is employed to regulate both the structural and morphological properties of Pt-based electrocatalysts which are expected to enhance the CO2 conversion reaction and increase catalytic reaction sites respectively. This bottom-up design of efficient catalysts synthesis strategy offers a rapid, cost-effective, and controllable approach to maximizing catalytic sites for CO<sub>2</sub> conversion under restricted catalyst loading. Also, this strategy showcases versatility across a broad spectrum of catalyst-based energy conversion and storage systems. With restricted areal mass loading of Pt catalyst, the as-developed porous electrocatalyst exhibits superior electrochemical performance over currently reported studies including low overpotential (< 0.5 V), excellent rate performance (up to 1.6 C, 1 C = 100  $\mu$ A cm<sup>-2</sup>), and high stability under elevated current density (over 200 cycles under 0.4 C). Moreover, stacked Li-CO2 pouch cells can be fabricated and operated under more practical operation conditions (280 mAhcell, and cycled at 0.2 C with over-potential < 0.6 V).

## 2. Structural regulation and engineering for Pt catalyst

According to previous studies, the reaction process in platinumbased LCBs can be described with the following reversible equations:  $3CO_2 + 4Li \leftrightarrow 2Li_2CO_3 + C$  (Fig. 1a). DFT calculations were first conducted to compare the electrocatalytic CO<sub>2</sub> reduction reaction (CO<sub>2</sub>RR) and CO2 evolution reaction (CO2ER) activity on different orientations of Pt. In the typical CO<sub>2</sub>RR process, the most important parameters to evaluate the LCBs performance are the adsorption of the reactant (CO<sub>2</sub>) and lithium ions) and the reaction product (Li<sub>2</sub>CO<sub>3</sub> and C). The CO<sub>2</sub> conversion kinetics is mainly dominated by catalysts in LCBs, as the supporting carbon matrix (e.g., carbon paper, carbon cloth.) generally exhibits poor catalytic performance toward CO2 conversion [23]. The adsorption energy of CO<sub>2</sub>, Li<sup>+</sup> and Li<sub>2</sub>CO<sub>3</sub> on typical thermodynamically stable surfaces (i.e. (111), (200) and (220)) of Pt are calculated (adsorption configuration in Fig. 1b). For the CO<sub>2</sub> reactant, Pt (111) facet exhibits the largest adsorption energies (-0.43 eV) compared with (200) and (220) facets as shown in Fig. 1c. Meanwhile, the adsorption energy for  $Li^+$  on Pt (111) facet (-1.12 eV) is much higher than that of the other two facets, which indicates the higher lithiophilicity on the Pt (111) facet. Thus, from the reactant perspective, Pt (111) exhibits the best compatibility and adsorption toward CO2 and Li+, indicating a larger concentration of reactants on the catalyst surface to promote higher CO<sub>2</sub>RR activity [24]. The adsorption behaviour of the main reaction product (Li<sub>2</sub>CO<sub>3</sub>) is further calculated, Pt (111) exhibits larger adsorption energy of -1.53 eV than (200) and (220) facets. In this case, Li<sub>2</sub>CO<sub>3</sub> can be more easily generated on Pt (111), leading to an enhanced reaction activity for potentially higher rate and capacity performance

The sluggish decomposition of Li<sub>2</sub>CO<sub>3</sub> has been considered the rate-determining step for the CO<sub>2</sub>ER process in LCBs. The large overpotential for the decomposition of Li<sub>2</sub>CO<sub>3</sub> during CO<sub>2</sub>ER greatly reduces the energy efficiency and further results in limited cycle life owing to the incomplete decomposition of discharging product and electrolyte instability under high charging potential [16,22]. A low decomposition energy barrier of Li<sub>2</sub>CO<sub>3</sub> could promote its complete decomposition, thus improve the cycling stability of the battery. The decomposition barrier of Li<sub>2</sub>CO<sub>3</sub> (C + Li<sub>2</sub>CO<sub>3</sub>  $\rightarrow$ Li<sup>+</sup> + LiC<sub>2</sub>O<sub>3</sub> + e) is evaluated as shown in Fig. 1d. As a result, Pt (111) also exhibits the lowest decomposition energy of Li<sub>2</sub>CO<sub>3</sub> (1.09 eV) among the three typical facets, hence in

favour of  $\text{Li}_2\text{CO}_3$  dissociation. According to the above theoretical calculations, Pt (111) has been identified as the most active interfacial facet to catalyse both  $\text{CO}_2\text{RR}$  and  $\text{CO}_2\text{ER}$  for LCBs.

High-temperature shock (HTS), as a non-equilibrium extreme method based on the electrical Joule heating, has been regarded as a low cost and highly efficient technique to regulate morphology and structure properties of diverse functional nanomaterials [26,27]. Next, we employed HTS technique to regulate the crystal orientation and exposed active sites on Pt catalysts (Fig. S1). Carbon cloth (Fig. S2) with good conductivity, flexibility and porosity was used as the electrode substrate [23,28]. Firstly, Pt was uniformly deposited on the carbon cloth (CC) via thermal evaporation (Fig. S3), and the resulting areal mass loading of Pt is  $\sim 0.1 \ \text{mg cm}^{-2}$ . The Pt-coated carbon cloth (pristine-Pt@CC) was further loaded on the HTS holder (Fig. S4) and thermal-treated under vacuum conditions with a cut-off heating temperature of 1500 °C (Fig. S5).

After 2 s of HTS process, the loaded Pt melted during the rapid temperature rise, and then self-assembled into nanoparticles during the abrupt temperature drop [29]. Transmission electron microscopy (TEM) observation identified the existence of nanoparticles with a size range of 5-10 nm (Fig. S6). The structural information of different air electrodes was investigated by X-ray diffraction (XRD) as shown in Fig. 1e. The broad peak at around 26° in all three electrodes can be ascribed to the carbon fibre of the CC substrate. After the Pt deposition, weak Pt peaks at (39.9°) can be identified according to the standard PDF cards (01-070-20057) [30]. In sharp contrast, the (111) peak was greatly intensified after the HTS treatment, indicating the successful implementation of the preferred orientation of Pt (111) which was demonstrated by TEM [31,32]. Besides, XRD patterns with fitting data (Fig. S7) showed a significantly increased content of (111) facet from 48.6 % to 63.6 % and the narrowed full width high maximum values also suggested larger crystalline grains. The lattice spacing of 0.225 nm can be observed, corresponding to the (111) crystal plane of Pt, which is also confirmed by the speckle rings of the selected area electron diffraction pattern (Fig. 1f) [33,34]. With more observation of other nanoparticles, it was found that the Pt (111) orientations dominated the surface of nanoparticle platinum (Fig. S8). To elucidate the As origin of preferred Pt (111) orientation during HTS process, surface energies of (111), (200) and (220) facets of Pt are compared in Fig. S9. Pt (111) facet exhibited the lowest surface energy (1.44 J  $\mathrm{m}^{-2}$ ) compared with (200) and (220) facets, which indicates that the (111) facet is a more thermodynamically stable facet. Thus, Pt (111) orientation exposed more during the abrupt cooling process [35]. Such approach could be adopted to synthesizing other metallic catalysts with desirable crystalline orientations.

Moreover, the dense thin-film morphology of the pristine Pt-coated electrode was transformed into a 3D porous structure (Fig. S10 and Fig. S11). The  $\rm N_2$  adsorption-desorption isotherm of the HTS-treated catalyst (Fig. S12) shows a typical hysteresis loop characteristic of a porous structure [36]. The introduced porosity not only significantly increased the specific surface area from 0.66 m² g $^{-1}$  to 1.25 m² g $^{-1}$  but also created hierarchical pore size distribution on the electrode surface [37]. Finite element method analysis was then employed to simulate the  $\rm CO_2$  flow on the surface of different electrodes (see Fig. S13 and Fig. S14 for detailed results). As a result, catalyst with porous structure allows faster CO<sub>2</sub> diffusion. In addition, such 3D porous catalyst structure is expected to promote electrolyte permeation and increase catalytic sites to facilitate CO<sub>2</sub> conversion.

# 3. Enhanced CO2 conversion kinetics and reversibility

After the Pt (111) preferred orientations and porous catalyst structure were successfully introduced in the air electrode, the  $CO_2$  conversion process was then evaluated in Li- $CO_2$  batteries under  $CO_2$  atmosphere (Fig. S15). The maximum areal capacity was first measured with a cut-off voltage at 2 V and under a current density of  $20~\mu A~cm^{-2}$  (Fig. S16). Notably, the porous-Pt-(111)@CC enabled a high areal

Nano Energy 117 (2023) 108872

capacity of 5.8 mAh cm<sup>-2</sup>, which is more than twice the capacity delivered by pristine-Pt@CC (2.6 mAh cm<sup>-2</sup>). To evaluate the utilization efficiency of Pt, the normalized specific areal capacity (areal capacity divided by the areal mass loading of Pt) is defined and compared with the reported literature as shown in Fig. S17. The porous-Pt-(111)@CC delivered the highest normalized specific areal capacity (58.1 Ah  $g_{catalyst}^{-1}$ ) with the minimum catalyst loading among all the listed catalysts (Table S2), suggesting a highly efficient utilization of the catalyst to promote CO2 conversion. Besides, the discharging voltage of porous-Pt-(111)@CC also outperforms pristine-Pt@CC under the same operating condition. The significantly improved areal capacity is contributed by the elevated specific surface and porous catalyst morphology that provide more available sites to accommodate the reaction product; meanwhile, higher contents of exposed preferred Pt (111) orientation accelerate CO2 conversion and product generation during the CO2RR process. Interestingly, distinctively different morphologies for the discharging product could be observed on porous-Pt-(111)@CC and pristine-Pt@CC (Fig. 2a and Fig. \$18). For pristine-Pt@CC, the discharging products tend to form isolated micro-sized particles following the Volmer-Weber mode due to the lack of catalytic sites, leading to residual CO<sub>2</sub>RR products on the electrode surface (Fig. S19). As illustrated in Fig. 2b, Benefiting from abundant and highly efficient catalytic sites, thin-film products are formed on porous-Pt-(111)@CC following the Frank-van der Merwe mode which can easily decompose upon the charging process (Fig. S20) [38].

The cyclic voltammetry (CV) tests (Fig. S21) of the Li-CO<sub>2</sub> batteries were conducted at the scan rate of 1 mV s<sup>-1</sup> within the potential range from 2.0 to 3.5 V to observe the redox reaction process for different electrocatalysts. The cathodic peaks started at 2.5 V corresponding to the Li<sub>2</sub>CO<sub>3</sub> and carbon formation during the CO<sub>2</sub>RR process. And during the anodic scanning, the peaks started at 2.8 V can be ascribed to the decomposition of the discharging product. The porous Pt catalyst

showed a larger reaction current and lower overpotential during charging compared with the pristine Pt catalyst and pure carbon electrode (CC) (Fig. S22), indicating an enhanced CO<sub>2</sub> utilization during CO<sub>2</sub>RR and facilitated decomposition of reaction product during CO<sub>2</sub>ER. Galvanostatic charging and discharging tests were carried out as shown in Fig. 2c. To make a better comparison with recent LCB literature, the cut-off capacity was accordingly set as 100  $\mu$ Ah cm $^{-2}$ . Considering the practical application of LCBs, a moderate operating current density of 40  $\mu$ A cm $^{-2}$  was applied. Porous-Pt-(111)@CC exhibits a charging plateau of 3.08 V with an overpotential of merely 0.65 V, which is one of the lowest values among all reported electrocatalysts (excluding the photoelectrocatalyst or redox mediator works) in LCBs under the same current density.

Since the reaction kinetics of  $CO_2RR$  and  $CO_2ER$  have a great impact on reversibility, electrochemical impedance spectra (EIS) were recorded during cycling to evaluate the overall reversibility of LCBs. The generation of reaction product during discharging will passivate the electrode, hence increasing the interfacial charge transfer resistance ( $R_{ct}$ ) for both catalysts (Fig. 2d and Table S1). Upon the charging process of the first cycle, the resistance recovered nearly to the pristine state before cycling for porous-Pt-(111)@CC, confirming the complete decomposition of the discharging product. By contrast,  $R_{ct}$  for pristine-Pt@CC was partially recovered at the charged state, indicating residual discharging product on the electrode.  $R_{ct}$  for pristine-Pt@CC became even higher after 10 cycles, suggesting a deteriorating interface, whereas porous-Pt-(111) @CC exhibited well-maintained interfacial resistance owing to the high reversibility.

To obtain the correlation between the componential information on electrode surfaces and the cell reversibility, LCBs under different states of charge were disassembled for ex-situ interfacial spectroscopy analysis. The ex-situ XPS (Fig. S23 and Fig. 3a) analysis of both catalysts exhibit distinctive Li<sub>2</sub>CO<sub>3</sub> signals in both C 1 s (290.3 eV) and Li 1 s

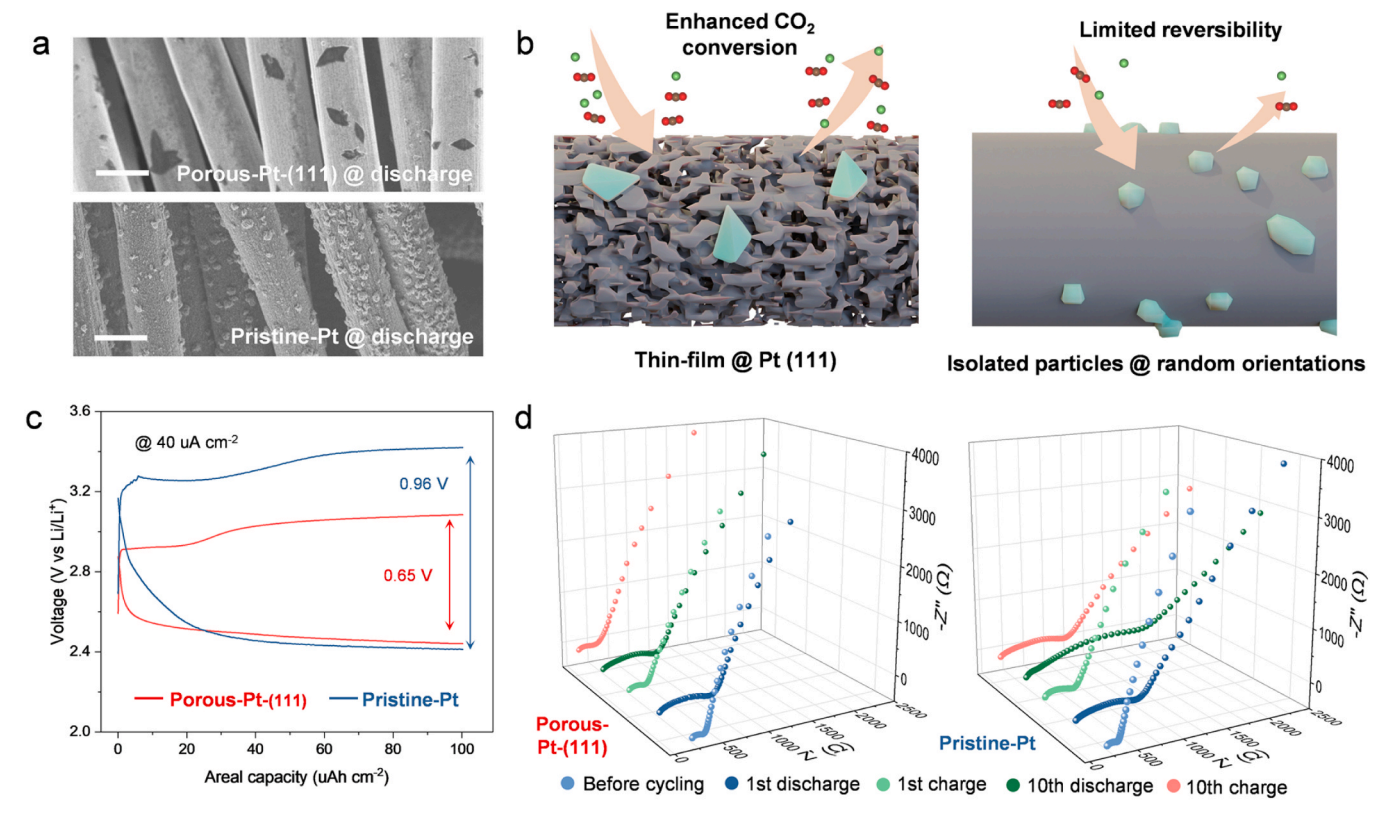


Fig. 2. Enhanced  $CO_2$  conversion and reversibility for Li- $CO_2$  battery. (a) Electrode morphology at discharging state (scale bar =  $10 \mu m$ ). (b) Schematic illustration of the different  $CO_2$  conversion processes on the catalysts. (c) Galvanostatic charge/discharge curves under the current density of  $40 \mu A cm^{-2}$ . (d) EIS spectra during cycling.

S. Chen et al. Nano Energy 117 (2023) 108872

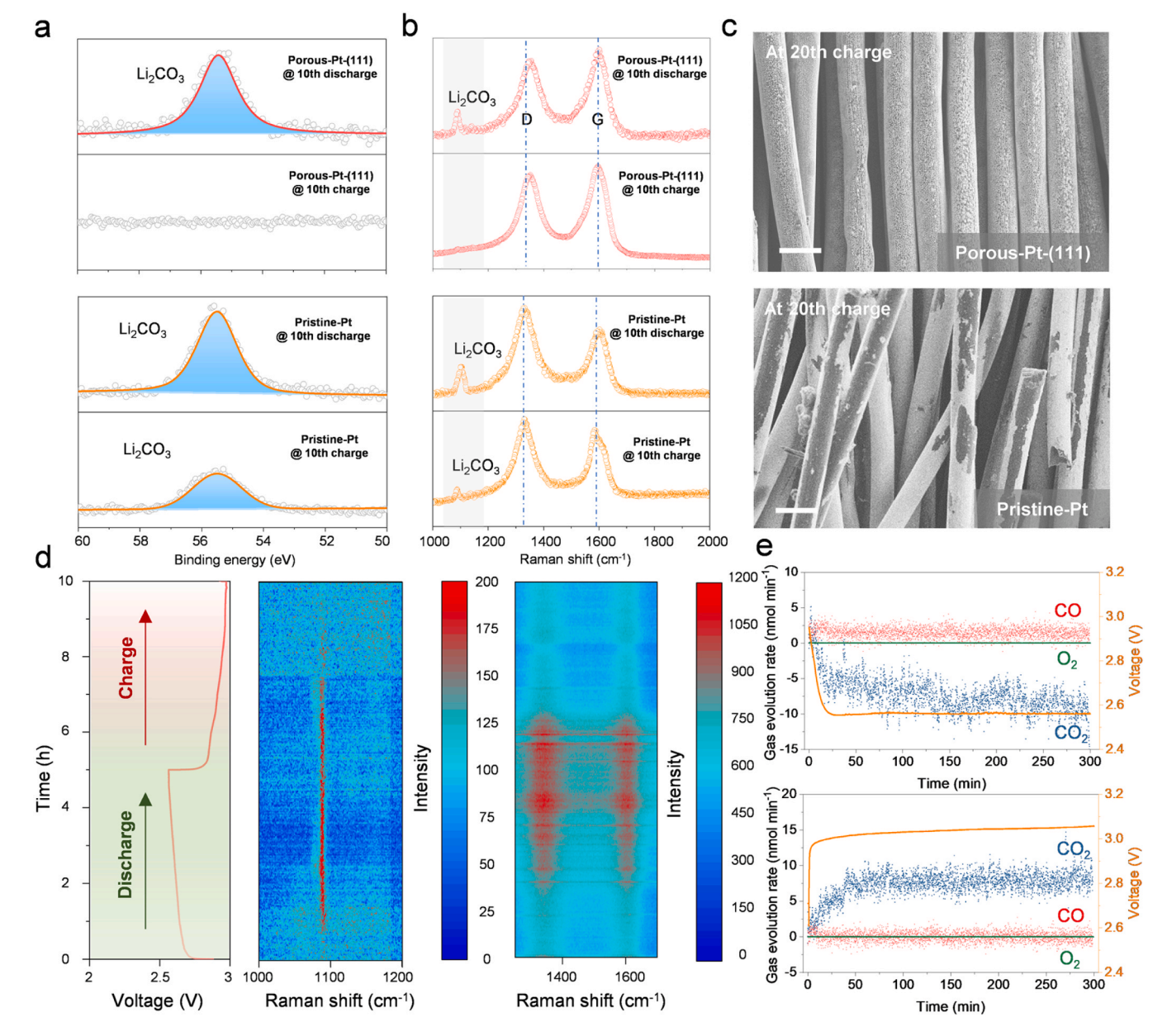


Fig. 3. Characterizations of the reversibility. (a) Li 1 s XPS spectra for air electrodes under different electrochemical status: discharge state and charge state. (b) Ex-situ Raman analysis of the cycled air electrodes. (c) SEM images of different electrodes after 20 cycles (scale bar =  $10 \mu m$ ). (d) In-situ Raman characterization of the porous Pt electrode. (e) Gas evolution during cycling of porous Pt electrode.

spectra (55.5 eV) at discharged state, confirming the generation of Li<sub>2</sub>CO<sub>3</sub> [36,39]. In the following charging process, all signals belonging to Li<sub>2</sub>CO<sub>3</sub> disappeared on porous-Pt-(111)@CC, suggesting the complete decomposition of Li<sub>2</sub>CO<sub>3</sub>. However, partial Li<sub>2</sub>CO<sub>3</sub> could still be detected on pristine-Pt@CC at charged state. Ex-situ Raman (Fig. 3b) and FTIR (Fig. S24) were also employed to reveal the reversibility of the catalyst-dependent CO<sub>2</sub> conversion. Consistent with the XPS measurement, porous-Pt-(111)@CC enhanced the reversible decomposition of discharging product Li<sub>2</sub>CO<sub>3</sub> as confirmed by the evolution of typical Raman stretching peaks ( $\sim$ 1090 cm<sup>-1</sup>) and FTIR spectra ( $\sim$ 1510 cm<sup>-1</sup>) [40–43]. Besides, XRD measurements for different electrochemistry states were analysed (Fig. S25). It could be observed that the characteristic peak (21.34°, 30.64° and 31.79°) of Li<sub>2</sub>CO<sub>3</sub> disappeared in the charging state on porous-Pt-(111)@CC [10].

It is reported that the nanostructure of the catalyst can affect the growth/evolution of discharging product on the catalyst surface [36, 38]. In return, the repeated catalytic behaviour will also introduce

reaction stress and change the catalyst structure [44,45]. The accumulation of incompletely decomposed discharge product will passivate the catalyst surface and worse still lead to catalyst structural collapse or detachment from the substrate owing to the residue stress [44,46]. The disassembled air electrodes were also observed by scanning electron microscope (SEM) (Fig. 3c). Surprisingly, the air electrode with pristine Pt catalyst suffered severe structure destruction. The pristine Pt catalyst was peeled off the carbon fibre and the non-active carbon substrate was exposed. While in the air electrodes with porous Pt catalyst, the structural integrity was maintained stable during cycling with the porous Pt catalyst structure well preserved. Based on the above results, it can be concluded that porous-Pt-(111)@CC facilitates the complete decomposition of thin film discharging product during charging owing to abundant and highly efficient catalytic sites, hence improve the excellent electrochemical reversibility. The porous structure is also beneficial to the dissipation of the reaction stress to maintain electrode structure integrity (Fig. 3c); while the residual Li<sub>2</sub>CO<sub>3</sub> on pristine-Pt@CC

S. Chen et al. Nano Energy 117 (2023) 108872

gradually accumulates, and eventually causes structure disintegration of the electrode owing to Pt detachment from the substrate. Furthermore, the SEM results of porous-Pt-(111)@CC after long-term cycling also confirmed the improved reversibility of  $\text{Li}_2\text{CO}_3$  decomposition (Fig. S26).

For further insights into the role of porous-Pt-(111)@CC in enhancing CO<sub>2</sub> conversion kinetics and reversibility, in-situ Raman and differential electrochemical mass spectrometry (DEMS) were conducted to probe the reaction mechanism. As shown in Fig. 3d, the Raman intensity of reaction product Li<sub>2</sub>CO<sub>3</sub> (typical peak at  $\sim\!1090~\text{cm}^{-1}$ ) and carbon (G-bond at  $\sim\!1600~\text{cm}^{-1}$  and D-bond at  $\sim\!1350~\text{cm}^{-1}$ ) was recorded [47]. During the galvanostatic discharging process, the intensity of the reaction products gradually increased. In the following charging process, the corresponding intensity gradually vanished. This result indicates that apart from Li<sub>2</sub>CO<sub>3</sub>, the evolution of C is also reversible. indicating superior reversibility. DEMS results (Fig. 3e) show that CO<sub>2</sub> was the only gas specie that being consumed/released during discharging/charging. The charge evolution during discharging or charging is  $2.93\times10^{-6}\text{mol}$  (20  $\mu\text{A}$  cm $^{-2}$ ). The molar

amounts of the consumed and released  $CO_2$  based on DEMS are calculated to be  $2.192 \times 10^{-6}~$  mol and  $2.183 \times 10^{-6}~$  mol for discharging and charging process, respectively. The  $CO_2$  mass-to-charge ratio during discharging or charging is very close to 0.75, indicating a highly reversible pathway ( $3CO_2 + 4Li^+ \leftrightarrow 2Li_2CO_3 + C$ ). Since irreversible Li-CO $_2$  reaction has been reported to generate  $O_2$  upon charging process as the following reaction path:  $2Li_2CO_3 \rightarrow 2CO_2 + O_2 + 4Li^+ + 4e^-$  [11,12], this result has ruled out the above mentioned  $Li_2CO_3$  decomposition route and further confirmed the high reversibility of  $CO_2$  conversion on porous-Pt-(111)@CC.

# 4. Electrochemical performance under more practical operating conditions

As previously mentioned, the real application of LCBs relies on their performance under practical current densities. Herein, additional electrochemical tests were carried out to evaluate the battery performance of porous-Pt-(111)@CC. Porous-Pt-(111)@CC exhibited a steady discharging/charging plateau under various current densities (Fig. 4a) and

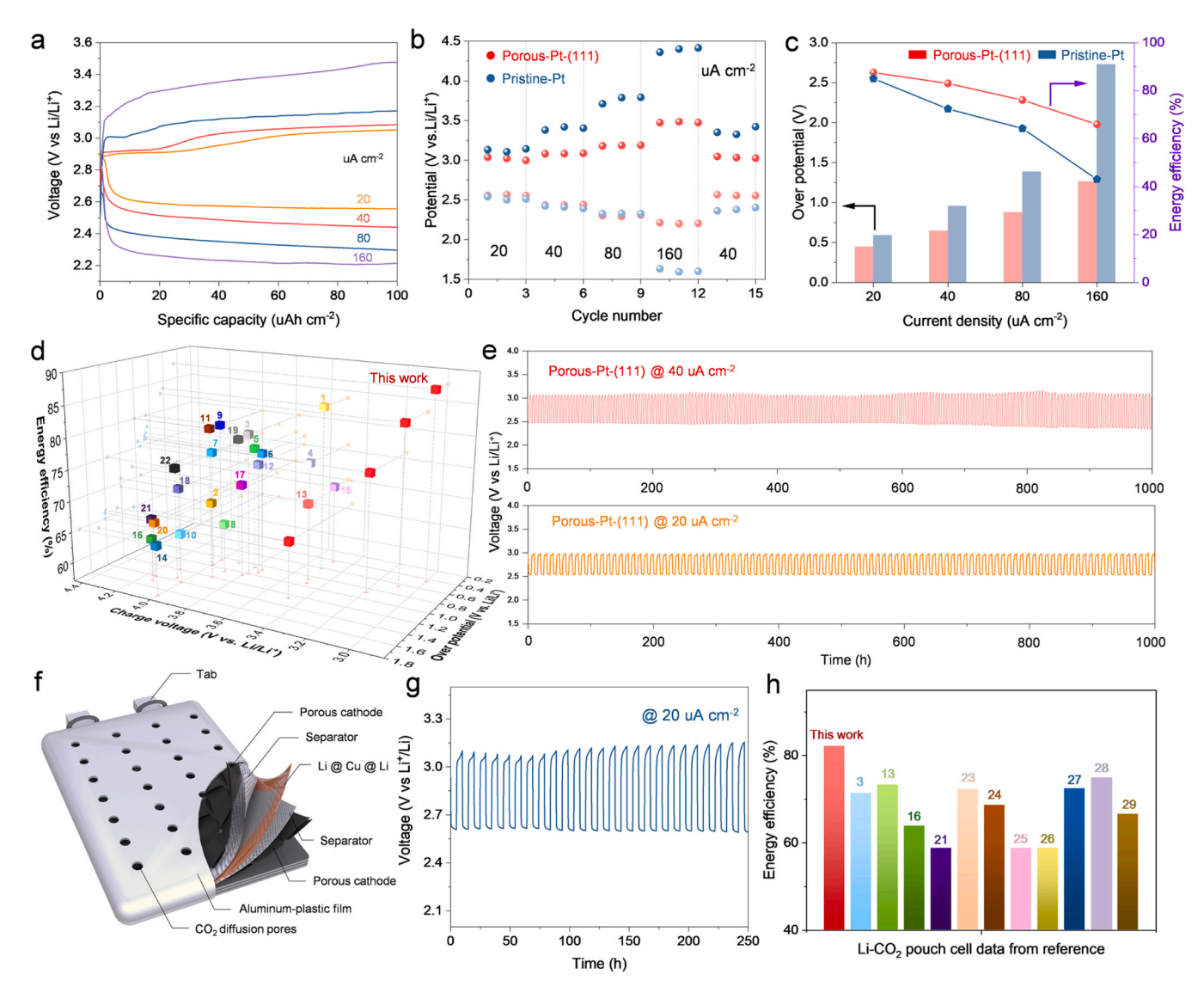


Fig. 4. Electrochemical performance under practical operating conditions. (a) Voltage-capacity curves under different current densities of porous Pt catalyst, the cut-off capacity of 100 μAh cm $^{-2}$ . (b) Charging/discharging voltage under different current densities for different catalysts. (c) Overpotential and energy efficiency under different current densities for different catalysts. (d) Comparison of LCB coin cell performance with literature from Table S2. (e) Long cycle performance of porous Pt catalyst-based LCB, under current densities of 20 μA cm $^{-2}$  and 40 μA cm $^{-2}$ . (f) Stacked structure of LCB pouch cell. (g) Cycle performance of the stacked LCB pouch cell under 20 μA cm $^{-2}$ . (h) Energy efficiency comparison of the Li-CO $_2$  pouch cell performance with literature from Table S3.

small overpotentials (Fig. 4b) of 0.45 V, 0.65 V, 0.89 V and 1.26 V at 20, 40, 80 and 160  $\mu$ A cm<sup>-2</sup>, respectively, which correspond to energy efficiencies (Fig. 4c) of 87.5 %, 82.1 %, 75.6 % and 65.9 %. In comparison, pristine-Pt@CC exhibited much poorer rate capabilities. The charging voltage of pristine-Pt@CC increased sharply (as high as 4.5 V) with the current density (Fig. S27 and Fig. 4b), resulting in inferior energy efficiencies of 85.0 %, 71.9 %, 63.7 % and 42.4 % at 20, 40, 80 and 160 µA cm<sup>-2</sup>, respectively. To further highlight the excellence of the asdeveloped porous Pt catalyst, the electrochemical performances (including charging voltage, overpotential and energy efficiency) were compared with previously reported Li-CO2 battery cathode catalysts as summarised in Fig. 4d and Table S2. Porous-Pt-(111)@CC clearly demonstrates the highest energy efficiency and lowest overpotential among all the listed metal or metal-based catalysts even under higher current densities (Fig. S28). Notably, the as-developed Pt catalyst with optimized catalytic sites also delivered the highest energy efficiency with the minimum areal mass loading compared with previously reported works (Fig. S29), indicating a much improved catalyst utilization

Owing to the sluggish CO<sub>2</sub> conversion kinetics, many reported LCBs are normally cycled at impractically low areal current densities (Fig. S28). Here, the cycle stability of the LCBs with different electrocatalysts was investigated at the current densities of 20 µA cm<sup>-2</sup> and 40 μA cm<sup>-2</sup>. As shown in Fig. S30, pristine-Pt@CC delivered a poor cycle performance under 40 µA cm<sup>-2</sup>. The charging voltage already reached 3.5 V within the first 10 cycles and gradually increased up to 4.5 V during sequential cycles. Worse still, the discharging voltage also dropped below 1.5 V, leading to disastrous energy efficiencies. The pure carbon electrode exhibited even poorer cycle performance as shown in Fig. S31. Remarkably, excellent cycle stability was exhibited by porous-Pt-(111)@CC as shown in Fig. 4e. Under current densities of 20  $\mu$ A cm<sup>-2</sup>, the as-assembled LCBs can be stably cycled for over 100 cycles (> 1000 h) with an average low overpotential of 0.5 V. Under the elevated current density of 40  $\mu A$  cm<sup>-2</sup>, LCBs based on the porous-Pt-(111) catalyst can be cycled over 1000 h (corresponding to over 200 cycles) with high energy efficiency of over 80 % (Fig. S32), evidencing that the high-rate performance and cycling stability can be simultaneously achieved by porous-Pt-(111)@CC. The porous-Pt-(111) catalyst based LCBs were further operated under higher specific areal capacity (200 µAh cm<sup>-2</sup>). Low overpotential (Fig. S33) and stable cycle performance (Fig. S34) remained demonstrating the enhanced CO2 conversion kinetics.

Single-layer Li-CO2 pouch cells have been previously reported, but many of them can only power low-energy or low-power electronics with the limited practical operation [37,48-50]. Developing practical pouch-cell-level Li-CO<sub>2</sub> batteries puts forward a challenging opportunity to realise the potential CO2 utilisation and energy storage ability of Li-CO<sub>2</sub> batteries. Here, to further demonstrate the potential of porous-Pt-(111)@CC in practical application proof-of-concept stacked Li-CO2 pouch cells (Fig. 4f) with two layers of air electrodes were assembled and tested. Under the current densities of 20  $\mu A$  cm<sup>-2</sup>, the stacked Li-CO<sub>2</sub> pouch cell delivered a total capacity of 280 mAh<sub>cell</sub> (Fig. S35). Apart from lighting the LED arrays as shown in Fig. S36, the as-developed stacked Li-CO<sub>2</sub> pouch cell can be stably cycled under 20  $\mu$ A cm<sup>-2</sup> (Fig. 4g) with low overpotential (0.5 V) and high energy efficiency (82.2 %) (Fig. S37). Compared with the reported Li-CO<sub>2</sub> pouch cells (Fig. 4h, Fig. S38 and Table S3), the stable cycling of the porous Pt based stacked Li-CO2 pouch cells with low overpotential and high energy efficiency demonstrates its potential for large scale application. Considering the utilization cost, the Pt/Carbon weight ratio in our cathode electrode is calculated to be 0.77 wt% which is only one-fourth of that in the commercial Pt/C catalyst (3 wt%). Meanwhile, no harmful or expensive chemicals are used during the synthesis process. Overall, compared with the traditional wet chemistry routine to synthesis electrocatalyst, the proposed catalyst regulation strategy not only provides a rapid, cost-effective, and controllable approach to

enhance the LCBs, but also inspires synthesis of catalysts based on non-noble metals. Furthermore, through the strategy of simultaneously tuning the crystalline facets and morphology, catalysts that previously considered ineffective might be revived.

### 5. Conclusions

In summary, following the theoretical identification of the highly efficient catalytic orientation of platinum catalyst toward CO2 conversion for LCBs, a porous Pt catalyst (porous-Pt-(111)@CC) with preferred orientation of (111) has been controllably and efficiently developed by fast electrical joule heating techniques. Benefiting from the improved CO<sub>2</sub> conversion kinetics on the (111) facet (including compatibility and affinity toward reactant, and the lower energy barrier for Li<sub>2</sub>CO<sub>3</sub> decomposition), porous-Pt-(111)@CC delivered remarkable electrochemical performance with minimum catalyst loading. Areal capacity could be doubled owing to the porous structure that with abundant catalytic reaction sites to accommodate reaction products. Ex-situ and in-situ characterizations have confirmed the high reversibility of the asdeveloped porous pt catalyst, which ensures the stable long-term cycling of LCBs with low overpotential and ultrahigh energy efficiency, outperforming most reported metal or metal-based electrocatalysts for LCBs. A proof-of-concept stacked Li-CO2 pouch cells are further fabricated and delivered considerable areal capacity and stable cycle performance under 0.2 C, demonstrating its potential in practical use. The proposed strategy to regulate specific catalytic sites and consequently maximize the utilization of catalysts provides a rational and eco-efficient approach for the synthesis of advanced catalysts toward next-generation high-performance energy conversion and storage devices.

### CRediT authorship contribution statement

Shiming Chen: Data curation, Formal analysis, Writing – original draft, Visualization. Kai Yang: Data curation, Formal analysis, Writing – original draft, Visualization, Writing – review & editing, Supervision. Hengyao Zhu: Data curation, Methodology. Jianan Wang: Resources. Yi Gong: Resources. Huanxin Li: Investigation. Manman Wang: Resources. Wenguang Zhao: Resources. Yuchen Ji: Resources. Feng Pan: Supervision, Funding acquisition. S. Ravi P. Silva: Conceptualization, Resources, Writing – review & editing. Yunlong Zhao: Writing – review & editing, Funding acquisition. Luyi Yang: Methodology, Writing – review & editing, Supervision, Project administration, Funding acquisition.

# **Declaration of Competing Interest**

The authors declare that they have no known competing financial interests or personal relationships that could have appeared to influence the work reported in this paper.

# Data availability

Data will be made available on request.

### Acknowledgements

L. Y. acknowledge the support from Shenzhen Science and Technology Research Grant (No. ZDSYS201707281026184). K.Y and Y.Z. acknowledge support from the EPSRC New Investigator Award (EP/V002260/1) and the Faraday Institute - Battery Study and Seed Research Project (FIRG052).

# Appendix A. Supporting information

Supplementary data associated with this article can be found in the online version at doi:10.1016/j.nanoen.2023.108872.

#### References

- [1] T. Ahmad, S. Liu, M. Sajid, K. Li, M. Ali, L. Liu, W. Chen, Electrochemical CO<sub>2</sub> reduction to C<sub>2+</sub> products using Cu-based electrocatalysts: a review, Nano Res. Energy 1 (2022), e9120021, https://doi.org/10.26599/NRE.2022.9120021.
- [2] J.-J. Wang, X.-P. Li, B.-F. Cui, Z. Zhang, X.-F. Hu, J. Ding, Y.-D. Deng, X.-P. Han, W.-B. Hu, A review of non-noble metal-based electrocatalysts for CO<sub>2</sub> electroreduction, Rare Met. 40 (11) (2021) 3019–3037, https://doi.org/10.1007/s12598-021-01736-x.
- [3] Z. Xie, X. Zhang, Z. Zhang, Z. Zhou, Metal–CO<sub>2</sub> batteries on the road: CO<sub>2</sub> from contamination gas to energy source, Adv. Mater. 29 (15) (2017), 1605891, https:// doi.org/10.1002/adma.201605891.
- [4] J. Wang, B. Marchetti, X.-D. Zhou, S. Wei, Heterogeneous electrocatalysts for metal–CO<sub>2</sub> batteries and CO<sub>2</sub> electrolysis, ACS Energy Lett. (2023) 1818–1838, https://doi.org/10.1021/acsenergylett.2c02445.
- [5] H. Han, S. Jin, S. Park, Y. Kim, D. Jang, M.H. Seo, W.B. Kim, Plasma-induced oxygen vacancies in amorphous MnOx boost catalytic performance for electrochemical CO<sub>2</sub> reduction, Nano Energy 79 (2021), 105492, https://doi.org/ 10.1016/j.nanoen.2020.105492.
- [6] Z. Wang, B. Liu, X. Yang, C. Zhao, P. Dong, X. Li, Y. Zhang, K. Doyle-Davis, X. Zeng, Y. Zhang, X. Sun, Dual catalytic sites of alloying effect bloom CO<sub>2</sub> catalytic conversion for highly stable Li–CO<sub>2</sub> battery, Adv. Funct. Mater. 33 (28) (2023), 2213931, https://doi.org/10.1002/adfm.202213931.
- [7] J. Choi, S. Park, H. Han, M. Kim, M. Park, J. Han, W.B. Kim, Highly efficient CO<sub>2</sub> electrolysis to CO on Ruddlesden-Popper perovskite oxide with in situ exsolved Fe nanoparticles, J. Mater. Chem. A 9 (13) (2021) 8740–8748, https://doi.org/10.1039/D0TA11328.J.
- [8] S. Zhang, L. Sun, Q. Fan, F. Zhang, Z. Wang, J. Zou, S. Zhao, J. Mao, Z. Guo, Challenges and prospects of lithium—CO<sub>2</sub> batteries, Nano Res. Energy 1 (2022), e9120001, https://doi.org/10.26599/NRE.2022.9120001.
- [9] W. Huang, J. Qiu, Y. Ji, W. Zhao, Z. Dong, K. Yang, M. Yang, Q. Chen, M. Zhang, C. Lin, K. Xu, L. Yang, F. Pan, Exploiting cation intercalating chemistry to catalyze conversion-type reactions in batteries, ACS Nano 17 (6) (2023) 5570–5578, https://doi.org/10.1021/acsnano.2c11029.
- [10] Y. Liu, R. Mao, B. Chen, B. Lu, Z. Piao, Y. Song, G. Zhou, H.-M. Cheng, Atomic design of bidirectional electrocatalysts for reversible Li-CO<sub>2</sub> batteries, Mater. Today (2023), https://doi.org/10.1016/j.mattod.2022.12.008.
- [11] J. Lin, W. Song, C. Xiao, J. Ding, Z. Huang, C. Zhong, J. Ding, W. Hu, A comprehensive overview of the electrochemical mechanisms in emerging alkali metal–carbon dioxide batteries, Carbon Energy (2023), https://doi.org/10.1002/ cev2.313.
- [12] Y. Jiao, J. Qin, H.M.K. Sari, D. Li, X. Li, X. Sun, Recent progress and prospects of Li-CO<sub>2</sub> batteries: mechanisms, catalysts and electrolytes, Energy Storage Mater. 34 (2021) 148–170, https://doi.org/10.1016/j.ensm.2020.09.014.
- [13] J. Li, A. Dai, K. Amine, J. Lu, Correlating catalyst design and discharged product to reduce overpotential in Li-CO<sub>2</sub> batteries, Small 17 (48) (2021), 2007760, https://doi.org/10.1002/smll.202007760.
- [14] X. Mu, H. Pan, P. He, H. Zhou, Li–CO<sub>2</sub> and Na–CO<sub>2</sub> batteries: toward greener and sustainable, Electr. Energy Storage 32 (27) (2020), 1903790, https://doi.org/ 10.1002/adma.201903790.
- [15] Y. Xu, H. Gong, L. Song, Y. Kong, C. Jiang, H. Xue, P. Li, X. Huang, J. He, T. Wang, A highly efficient and free-standing copper single atoms anchored nitrogen-doped carbon nanofiber cathode toward reliable Li–CO<sub>2</sub> batteries, Mater. Today Energy 25 (2022), 100967, https://doi.org/10.1016/j.mtener.2022.100967.
- [16] J. Lin, J. Ding, H. Wang, X. Yang, X. Zheng, Z. Huang, W. Song, J. Ding, X. Han, W. Hu, Boosting energy efficiency and stability of Li-CO<sub>2</sub> batteries via synergy between Ru atom clusters and single-atom Ru-N4 sites in the electrocatalyst cathode, Adv. Mater. 34 (17) (2022), 2200559, https://doi.org/10.1002/pdc.202200559
- [17] R. Li, J. Xu, Q. Zhao, W. Ren, R. Zeng, Q. Pan, X. Yan, J. Ba, T. Tang, W. Luo, Cathodic corrosion as a facile and universal method for the preparation of supported metal single atoms, Nano Res. 15 (3) (2022) 1838–1844, https://doi. org/10.1007/s12274-021-3767-3.
- [18] C.D. Koolen, W. Luo, A. Züttel, From single crystal to single atom catalysts: structural factors influencing the performance of metal catalysts for CO<sub>2</sub> electroreduction, ACS Catal. 13 (2) (2023) 948–973, https://doi.org/10.1021/ acceptal 2003842
- [19] F. Lü, H. Bao, Y. Mi, Y. Liu, J. Sun, X. Peng, Y. Qiu, L. Zhuo, X. Liu, J. Luo, Electrochemical CO<sub>2</sub> reduction: from nanoclusters to single atom catalysts, Sustain. Energy Fuels 4 (3) (2020) 1012–1028, https://doi.org/10.1039/C9SE00776H.
- [20] G. Giannakakis, M. Flytzani-Stephanopoulos, E.C.H. Sykes, Single-atom alloys as a reductionist approach to the rational design of heterogeneous catalysts, Acc. Chem. Res. 52 (1) (2019) 237–247, https://doi.org/10.1021/acs.accounts.8b00490.
- [21] Z. Chen, J. Liu, M.J. Koh, K.P. Loh, Single-atom catalysis: from simple reactions to the synthesis of complex molecules, Adv. Mater. 34 (25) (2022), 2103882, https://doi.org/10.1002/adma.202103882.
- [22] A.K. Chourasia, A.D. Pathak, C. Bongu, K. Manikandan, S. Praneeth, K.M. Naik, C. S. Sharma, In situ/operando characterization techniques: the guiding tool for the development of Li–CO<sub>2</sub> battery, Small Methodes 6 (12) (2022), 2200930, https://doi.org/10.1002/smtd.202200930.

- [23] B. Lu, B. Chen, D. Wang, C. Li, R. Gao, Y. Liu, R. Mao, J. Yang, G. Zhou, Engineering the interfacial orientation of MoS<sub>2</sub>/Co<sub>9</sub>S<sub>8</sub> bidirectional catalysts with highly exposed active sites for reversible Li-CO<sub>2</sub> batteries, Proc. Natl. Acad. Sci. USA 120 (6) (2023), e2216933120, https://doi.org/10.1073/pnas.2216933120.
- [24] B. Chen, D. Wang, B. Zhang, X. Zhong, Y. Liu, J. Sheng, Q. Zhang, X. Zou, G. Zhou, H.-M. Cheng, Engineering the active sites of graphene catalyst: from CO<sub>2</sub> activation to activate Li-CO<sub>2</sub> batteries, ACS Nano 15 (6) (2021) 9841–9850, https://doi.org/ 10.1021/accepta.0.100756
- [25] B. Chen, D. Wang, J. Tan, Y. Liu, M. Jiao, B. Liu, N. Zhao, X. Zou, G. Zhou, H.-M. Cheng, Designing electrophilic and nucleophilic dual centers in the ReS<sub>2</sub> plane toward efficient bifunctional catalysts for Li-CO<sub>2</sub> batteries, J. Am. Chem. Soc. 144 (7) (2022) 3106–3116, https://doi.org/10.1021/jacs.1c12096.
- [26] Y. Yao, Z. Huang, P. Xie, S.D. Lacey, R.J. Jacob, H. Xie, F. Chen, A. Nie, T. Pu, M. Rehwoldt, D. Yu, M.R. Zachariah, C. Wang, R. Shahbazian-Yassar, J. Li, L. Hu, Carbothermal shock synthesis of high-entropy-alloy nanoparticles, Science 359 (6383) (2018) 1489–1494, https://doi.org/10.1126/science.aan5412.
- [27] S. Xu, G. Zhong, C. Chen, M. Zhou, D.J. Kline, R.J. Jacob, H. Xie, S. He, Z. Huang, J. Dai, A.H. Brozena, R. Shahbazian-Yassar, M.R. Zachariah, S.M. Anlage, L. Hu, Uniform, scalable, high-temperature microwave shock for nanoparticle synthesis through defect engineering, Matter 1 (3) (2019) 759–769, https://doi.org/10.1016/j.matt.2019.05.022.
- [28] Y. Jin, C. Hu, Q. Dai, Y. Xiao, Y. Lin, J.W. Connell, F. Chen, L. Dai, High-performance Li-CO<sub>2</sub> batteries based on metal-free carbon quantum dot/holey graphene composite catalysts, Adv. Funct. Mater. 28 (47) (2018), 1804630, https://doi.org/10.1002/adfm.201804630.
- [29] S. Liu, Y. Shen, Y. Zhang, B. Cui, S. Xi, J. Zhang, L. Xu, S. Zhu, Y. Chen, Y. Deng, W. Hu, Extreme environmental thermal shock induced dislocation-rich Pt nanoparticles boosting hydrogen evolution reaction, Adv. Mater. 34 (2) (2022), 2106973, https://doi.org/10.1002/adma.202106973.
- [30] M.K. Carpenter, T.E. Moylan, R.S. Kukreja, M.H. Atwan, M.M. Tessema, Solvothermal synthesis of platinum alloy nanoparticles for oxygen reduction electrocatalysis, J. Am. Chem. Soc. 134 (20) (2012) 8535–8542, https://doi.org/ 10.1021/ja300756y.
- [31] S.M. Geyer, R. Methaapanon, R. Johnson, S. Brennan, M.F. Toney, B. Clemens, S. Bent, Structural evolution of platinum thin films grown by atomic layer deposition, J. Appl. Phys. 116 (6) (2014), 064905, https://doi.org/10.1063/ 14892104
- [32] J. Zhu, D. Xiao, W. Peng, F. Lan, D. Wan, Influence of rapid thermal processing on the orientation properties of PbTiO<sub>3</sub> thin film, Cryst. Res. Technol. 32 (3) (1997) 449–453, https://doi.org/10.1002/crat.2170320312.
- [33] W. Wang, Z. Wang, M. Yang, C.-J. Zhong, C.-J. Liu, Highly active and stable Pt (111) catalysts synthesized by peptide assisted room temperature electron reduction for oxygen reduction reaction, Nano Energy 25 (2016) 26–33, https://doi.org/10.1016/j.nanoen.2016.04.022.
- [34] M. Wang, H. Liu, J. Ma, G. Lu, The activity enhancement of photocatalytic water splitting by F- pre-occupation on Pt(100) and Pt(111) co-catalyst facets, Appl. Catal. B: Environ. 266 (2020), 118647, https://doi.org/10.1016/j. aprath 2020 118647
- [35] C. Li, N. Clament Sagaya Selvam, J. Fang, Shape-controlled synthesis of platinum-based nanocrystals and their electrocatalytic applications in fuel cells, Nano-Micro Lett. 15 (1) (2023) 83, https://doi.org/10.1007/s40820-023-01060-2.
- [36] K. Wang, D. Liu, L. Liu, X. Li, H. Wu, Z. Sun, M. Li, A.S. Vasenko, S. Ding, F. Wang, C. Xiao, Isolated metalloid tellurium atomic cluster on nitrogen-doped carbon nanosheet for high-capacity rechargeable lithium-CO<sub>2</sub> battery, Adv. Sci. 10 (7) (2023), 2205959, https://doi.org/10.1002/advs.202205959.
- [37] Q. Deng, Y. Yang, C. Mao, T. Wang, Z. Fang, W. Yan, K. Yin, Y. Zhang, Electronic state modulation and reaction pathway regulation on necklace-like MnO<sub>x</sub>-CeO<sub>2</sub>@ polypyrrole hierarchical cathode for advanced and flexible Li-CO<sub>2</sub> batteries, Adv. Energy Mater. 12 (14) (2022), 2103667, https://doi.org/10.1002/aepm 202103667
- [38] J. Zhou, T. Wang, L. Chen, L. Liao, Y. Wang, S. Xi, B. Chen, T. Lin, Q. Zhang, C. Ye, X. Zhou, Z. Guan, L. Zhai, Z. He, G. Wang, J. Wang, J. Yu, Y. Ma, P. Lu, Y. Xiong, S. Lu, Y. Chen, B. Wang, C.-S. Lee, J. Cheng, L. Gu, T. Zhao, Z. Fan, Boosting the reaction kinetics in aprotic lithium-carbon dioxide batteries with unconventional phase metal nanomaterials, Proc. Natl. Acad. Sci. USA 119 (40) (2022), e2204666119, https://doi.org/10.1073/pnas.2204666119
- [39] L. Chen, J. Zhou, J. Zhang, G. Qi, B. Wang, J. Cheng, Copper indium sulfide enables Li-CO<sub>2</sub> batteries with boosted reaction kinetics and cycling stability, Energy Environ. Mater. 0 (2022) 1, <a href="https://doi.org/10.1002/eem2.12415">https://doi.org/10.1002/eem2.12415</a>.
  [40] P.-F. Zhang, T. Sheng, Y. Zhou, Y.-J. Wu, C.-C. Xiang, J.-X. Lin, Y.-Y. Li, J.-T. Li,
- [40] P.-F. Zhang, T. Sheng, Y. Zhou, Y.-J. Wu, C.-C. Xiang, J.-X. Lin, Y.-Y. Li, J.-T. Li, L. Huang, S.-G. Sun, Li-CO<sub>2</sub>/O<sub>2</sub> battery operating at ultra-low overpotential and low O<sub>2</sub> content on Pt/CNT catalyst, Chem. Eng. J. 448 (2022), 137541, https://doi. org/10.1016/j.cej.2022.137541.
- [41] Y. Jin, F. Chen, J. Wang, Achieving low charge overpotential in a Li-CO<sub>2</sub> battery with bimetallic RuCo nanoalloy decorated carbon nanofiber cathodes, ACS Sustain. Chem. Eng. 8 (7) (2020) 2783–2792, https://doi.org/10.1021/acssuschemeng.9b06668.
- [42] Y. Qiao, J. Yi, S. Wu, Y. Liu, S. Yang, P. He, H. Zhou, Li-CO<sub>2</sub> electrochemistry: a new strategy for CO<sub>2</sub> fixation and energy storage, Joule 1 (2) (2017) 359–370, https://doi.org/10.1016/j.joule.2017.07.001.

- [43] X. Zhang, T. Wang, Y. Yang, X. Zhang, Z. Lu, J. Wang, C. Sun, Y. Diao, X. Wang, J. Yao, Breaking the stable triangle of carbonate via W–O bonds for Li-CO<sub>2</sub> batteries with low polarization, ACS Energy Lett. 6 (10) (2021) 3503–3510, https://doi.org/10.1021/acsenergylett.1c01428.
- [44] Z.-Z. Shen, Y.-Z. Zhang, C. Zhou, R. Wen, L.-J. Wan, Revealing the correlations between morphological evolution and surface reactivity of catalytic cathodes in lithium—oxygen batteries, J. Am. Chem. Soc. 143 (51) (2021) 21604–21612, https://doi.org/10.1021/jacs.1c09700.
- [45] O. Keisar, Y. Ein-Eli, Y. Alfi, Y. Cohen, Insights into the surface and stress behavior of manganese-oxide catalyst during oxygen reduction reaction, J. Power Sources 450 (2020), 227545, https://doi.org/10.1016/j.jpowsour.2019.227545.
- [46] H. Dykes, Rosy, D. Sharon, M. Noked, Ö. Çapraz, In situ stress measurements on thin film Au positive electrode during the first discharge of Li-O<sub>2</sub> batteries, J. Electrochem. Soc. 168 (11) (2021), 110551, https://doi.org/10.1149/1945-7111/ac3937.
- [47] T. Jian, W. Ma, C. Xu, H. Liu, J. Wang, Intermetallic-driven highly reversible electrocatalysis in Li–CO<sub>2</sub> battery over nanoporous Ni<sub>3</sub>Al/Ni heterostructure, eScience (2023), 100114, https://doi.org/10.1016/j.esci.2023.100114.
- [48] G. Qi, J. Zhang, L. Chen, B. Wang, J. Cheng, Binder-free MoN nanofibers catalysts for flexible 2-electron oxalate-based Li-CO<sub>2</sub> batteries with high energy efficiency, Adv. Funct. Mater. 32 (22) (2022), 2112501, https://doi.org/10.1002/ adfm 202112501
- [49] Y. Wang, J. Zhou, C. Lin, B. Chen, Z. Guan, A.M. Ebrahim, G. Qian, C. Ye, L. Chen, Y. Ge, Q. Yun, X. Wang, X. Zhou, G. Wang, K. Li, P. Lu, Y. Ma, Y. Xiong, T. Wang, L. Zheng, S. Chu, Y. Chen, B. Wang, C.-S. Lee, Y. Liu, Q. Zhang, Z. Fan, Decreasing the overpotential of aprotic Li-CO<sub>2</sub> batteries with the in-plane alloy structure in ultrathin 2D Ru-based nanosheets, Adv. Funct. Mater. 32 (30) (2022), 2202737, https://doi.org/10.1002/adfm.202202737.
- [50] L. Liu, Y. Qin, K. Wang, H. Mao, H. Wu, W. Yu, D. Zhang, H. Zhao, H. Wang, J. Wang, C. Xiao, Y. Su, S. Ding, Rational design of nanostructured metal/C interface in 3D self-supporting cellulose carbon aerogel facilitating high-performance Li-CO<sub>2</sub> batteries, Adv. Energy Mater. 12 (20) (2022), 2103681, https://doi.org/10.1002/aenm.202103681.



Shiming Chen received his bachelor's degree from the Institute for Advanced Study, Nanchang University (China) in 2020. He is currently a PhD candidate under the supervision of Prof. Feng Pan in School of Advanced Materials, Peking University Shenzhen Graduate School, China. His research focuses on the anode materials of lithium-ion batteries and quantum chemical calculation.



Dr Kai Yang is a Lecturer in the Advanced Technology Institute at the University of Surrey. He received his PhD degree from the School of Advanced Materials at Peking University Shenzhen Graduate School in Prof. Feng Pan's group. His research interests mainly focus on developing in-situ characterizations for interfacial research in energy storage/conversion material and devices, developing composite solid electrolytes for SSBs, carbon dioxide fixation and utilization technologies such as Li/Na/Zn-CO $_2$  battery, and developing nanoelectronics platforms for energy applications.



Hengyao Zhu obtained his bachelor's degree from Beijing University of Aeronautics and Astronautics (China) in 2021. He is currently studying for the master's degree under the guidance of Prof. Feng Pan in the School of Advanced Materials, Peking University. His research interests include anode materials and theoretical calculations for lithium-ion batteries.



Dr Jianan Wang is currently an associate professor at Department of Environmental Science and Engineering at Xi'an Jiaotong University. He received his Ph. D. degree from School of Energy and Power Engineering at Xi'an Jiaotong University. His research interests include Li-ion/Li-S/Li-metal batteries, solid-state batteries, advanced energy storage technologies (including the development of high-performance commercial battery materials, battery integration and thermal management), and gas sensor technologies for environmental and battery monitoring.



Yi Gong is currently a PhD candidate at Advance Technology Institute (ATI), the University of Surrey. He received his master's degree from Hunan University in 2018. Between 2018 and 2020, he served as an R&D Engineer at the Changsha Mining Research Institute, China Minmetals, where he concentrated on the research for commercial applications of graphene. His current research interest focuses on design and fabrication of sensor device for battery diagnostics development of advanced materials for high energy density batteries.



**Dr Huanxin Li** is currently a Postdoctoral Researcher in the Department of Chemistry, University of Oxford. Prior to this, he was a Postdoctoral Research Associate in Department of Engineering, University of Cambridge. He carried out his doctoral training at the Department of Chemistry and Chemical Engineering, Hunan University (HNU) and the Department of Chemistry at King's College London (KCL), with the focus on electrochemical thermal cells and energy storage devices. Dr Li gained highly multidisciplinary research experience in materials science, electrochemistry, and batteries.



Wenguang Zhao is currently a PhD candidate at the School of Advanced Materials in Peking University under the supervision of Prof. Feng Pan. His primary research interests lie in lithiumrich materials and high-voltage lithium cobalt oxide materials.



Yuchen Ji is currently a PhD candidate at Peking University, Shenzhen Graduate School under the supervision of Prof. Feng Pan. He received his bachelor's degree from Beijing University of Technology in 2019. His research focuses on the in situ advanced characterization of the electrolyte and interface evolution in secondary batteries.



Prof. Feng Pan, Chair-Professor, VP Peking University Shenzhen Graduate School, Founding Dean of School of Advanced Materials, Director of National Center of Electric Vehicle Power Battery and Materials for International Research, received his bachelor's degree from Dept. Chemistry, Peking University in 1985 and Ph.D. from Dept. of P&A Chemistry, University of Strathclyde (UK). Prof. Pan has been engaged in fundamental research of structure chemistry, exploring "Material Gene" for Li-ion batteries and developing novel energy conversion- storage materials & devices.



Dr Yunlong Zhao is an Associate Professor at the Dyson School of Design Engineering, Imperial College London. He also holds a joint appointment at the National Physical Laboratory (UK) as a Senior Scientist. Dr Yunlong Zhao has developed a series of novel electrochemical energy devices, sensors, and their integration into 2D on-chip and 3D soft systems for the in-depth studies of electrochemistry, electrophysiology and healthcare, with over 90 publications and 9000 citations. His research interests include advanced electrochemical energy storage devices, bioelectronic devices/sensors, and integrated on-chip and 3D soft electronic systems.



**Prof. S. Ravi P. Silva CBE FREng** is a Distinguished Professor and Director of the Advanced Technology Institute at University of Surrey. He joined Surrey after completing undergraduate and postgraduate degrees at Cambridge. His research interests include energy materials, solar cells, and large-area electronics, which has resulted in over 650 journal papers with 28,000 citations. He has won research funding of £ 45 M, and is inventor of 45 patents. He is a Fellow of the Royal Academy of Engineering and a Fellow of the National Academy of Sciences Sri Lanka. He was made a Commander of the Order of the British Empire.



**Dr Luyi Yang** received his bachelor's degree from the Department of Chemistry at Xiamen University (China) in 2010 and earned PhD degree from the School of Chemistry at Southampton University (U.K.) in 2015. He is currently an associate research professor at the School of Advanced Materials, Peking University, Shenzhen Graduate School. His research interests mainly focus on the investigation of key materials in lithium-ion and sodium-ion batteries through advanced characterization techniques.